

THESIS FOR THE DEGREE OF LICENTIATE OF ENGINEERING

# On Filter and Code Design for Energy Efficient Fiber-Optic Communications

ALIREZA SHEIKH



**CHALMERS**

Department of Electrical Engineering  
Communication Systems Group  
CHALMERS UNIVERSITY OF TECHNOLOGY

Göteborg, Sweden 2017

# **On Filter and Code Design for Energy Efficient Fiber-Optic Communications**

ALIREZA SHEIKH

© ALIREZA SHEIKH, 2017.

Technical report number: R006/2017

ISSN 1403-266X

Department of Electrical Engineering  
Communication Systems Group  
CHALMERS UNIVERSITY OF TECHNOLOGY  
SE-412 96 Göteborg  
Sweden  
Telephone: +46 (0)31 – 772 1000  
Email: asheikh@chalmers.se

Typeset by the author using L<sup>A</sup>T<sub>E</sub>X.

Chalmers Reproservice  
Göteborg, Sweden 2017

# Abstract

The advent of the Internet not only changed the communication methods significantly, but also the life-style of the human beings. The number of Internet users has grown exponentially in the last decade, and the number of users exceeded 3.4 billion in 2016. Fiber links serve as the Internet backbone, hence, the fast grow of the Internet network and the sheer of new applications is highly driven by advances in optical communications. The emergence of coherent optical systems has led to a more efficient use of the available spectrum compared to traditional on-off keying transmission, and has made it possible to increase the supported data rates. Transmission over fiber suffers from several impairments, which can be compensated for to a large extent using sophisticated digital signal processing (DSP). This comes at the cost of increasing the receiver complexity, which in turn leads to a higher energy consumption. Therefore, improving the energy efficiency of fiber-optic systems is of utmost interest. In this thesis, we attempt to improve the energy efficiency of coherent optical systems from an algorithmic design perspective.

Chromatic dispersion (CD) is one of the major impairments that limits the transmission reach of optical systems. CD can be compensated for in the DSP of the receiver. To improve the energy efficiency of CD compensation, one should take implementation considerations into account when designing the CD compensation filter. In this thesis, we design a new CD compensation filter that is more robust to quantization errors. This allows to reduce the required word length for the filter implementation and the energy consumption of the CD compensation.

To achieve high spectral efficiencies and improve the transmission reach, coding in combination with a higher order modulation, a scheme known as coded modulation (CM), has become indispensable in fiber-optic communications. In the recent years, graph-based codes such as low-density parity-check codes and soft decision decoding (SDD) have been adopted for long-haul coherent optical systems. SDD yields very high net coding gains but at the expense of a high decoding complexity, which brings implementation challenges at very high data rates. Hard decision decoding (HDD) is an appealing alternative that reduces the decoding complexity. This motivates the focus on this thesis on HDD. In particular, we derive achievable information rates (AIRs) for CM with HDD for both bit-wise and symbol-wise decoding, and show that bit-wise HDD yields significantly higher AIRs. We also design nonbinary staircase codes using density evolution. Finite length simulation results of binary and nonbinary staircase codes corroborate the conclusions arising from the AIR analysis, i.e., for HDD binary codes are preferable.

**Keywords:** Achievable information rates, chromatic dispersion, coded modulation, filter design, hard decision decoding, nonbinary staircase codes.



# Preface

This thesis is in partial fulfillment for the degree of Licentiate of Engineering at Chalmers University of Technology.

The work resulting in this thesis was carried out between October 2014 and September 2017 at the Communication and Antenna Systems Division, Department of Electrical Engineering, Chalmers University of Technology. Professor Alexandre Graell i Amat is the main supervisor and the examiner. In addition, Professor Magnus Karlsson is the co-supervisor.

This work was funded by the Knut and Alice Wallenberg Foundation and the Swedish Research Council under grant 2016-04253.



# List of Publications

This thesis is based on the work contained in the following appended papers:

## Paper A

**A. Sheikh**, C. Fougstedt, A. Graell i Amat, P. Johannisson, P. Larsson-Edefors, and M. Karlsson, “Dispersion Compensation FIR Filter With Improved Robustness to Coefficient Quantization Errors,” *IEEE/OSA J. Lightw. Technol.*, vol. 34, no. 22, pp. 5110-5117, Nov. 2016.

## Paper B

**A. Sheikh**, A. Graell i Amat, and G. Liva, “Achievable Information Rates for Coded Modulation with Hard Decision Decoding for Coherent Fiber-Optic Systems,” submitted to *IEEE/OSA J. Lightw. Technol.*, Jun. 2017.

## Paper C

**A. Sheikh**, A. Graell i Amat, and M. Karlsson, “Nonbinary Staircase Codes for Spectrally and Energy Efficient Fiber-Optic Systems,” in Proc. *Optical Fiber Commun. Conf. (OFC)*, Los Angeles, CA, 2017.

*Other related publications of the author not included in this thesis:*

- **A. Sheikh**, C. Fougstedt, A. Graell i Amat, P. Johannisson, P. Larsson-Edefors, and M. Karlsson, “Dispersion Compensation Filter Design Optimized for Robustness and Power Efficiency,” in Proc. *Advanced Photonics*, Boston, MA, 2015.
- C. Fougstedt, **A. Sheikh**, P. Johannisson, A. Graell i Amat, and P. Larsson-Edefors, “Power-Efficient Time-Domain Dispersion Compensation Using Optimized FIR Filter Implementation,” in Proc. *Advanced Photonics*, Boston, MA, 2015.
- **A. Sheikh**, A. Graell i Amat, and G. Liva, “On Achievable Information Rates for Coherent Fiber-Optic Systems with Hard Decision Decoding,” in Proc. *European Conf. Optical Commun. (ECOC)*, Gothenburg, Sweden, 2017.
- **A. Sheikh**, A. Graell i Amat, and G. Liva, “Probabilistically-Shaped Coded Modulation with Hard Decision Decoding for Coherent Optical Systems,” in Proc. *European Conf. Optical Commun. (ECOC)*, Gothenburg, Sweden, 2017.
- **A. Sheikh**, A. Graell i Amat, and G. Liva, “Probabilistically-Shaped Coded Modulation with Hard Decision Decoding and Staircase Codes,” [Online]. Available: <http://arxiv.org/abs/1606.01689>
- C. Fougstedt, **A. Sheikh**, P. Johannisson, and P. Larsson-Edefors, “Filter Implementation for Power-Efficient Dispersion Compensation,” submitted to *IEEE Trans. Circuits and Systems*, Jul. 2017.



# Acknowledgment

This thesis is the result of spending countless hours in my office at Chalmers. I wish to thank all people who made this time productive and joyful.

First and for a most, I would like to express my deepest gratitude to my main supervisor, Prof. Alexandre Graell i Amat for his support, motivation, patience, and guidance during the last three years. Àlex, thanks for letting me exploring different topics and work on interesting research problems. Looking forward to continuing my PhD journey with you.

I wish also to thank my co-supervisor Prof. Magnus Karlsson for all fruitful discussions we had and all support he provided. I would also like to appreciate Prof. Erik Agrell and Prof. Peter Andrekson for their support in my project. Next, my heart-felt thanks goes to Dr. Gianluigi Liva for sharing his brilliant ideas. We spent a short time with each other, mostly via Skype, but very efficient time in terms of research outcome. I wish also to thank Dr. Pontus Johannisson for his guidance in the first year of my PhD.

I would also like to thank the head of the communication and antenna systems (CAS) division, Prof. Erik Ström for providing an awesome work place. Special thanks to Agneta and Natasha for helping with the administrative works. Thanks in general to all former and current members of the CAS and fiber-optic communications research centre. In particular, many thanks to Dr. Naga V. Irukulapati, Dr. Christian Häger, Christoffer, Cristian, Rahul, and Keerthi. A special thank to my buddy and office mate Kamran, for the technical and nontechnical discussions we had. Kamran, thanks for enduring the cold weather while I kept the window of the office open! Many thanks to Mehrzad and Mohammad for spending enjoyable time together and all you did for me.

I had a great time, being surrounded by my great friends in the large Iranian community at Chalmers. Special thanks to Samar, Fatemeh, Parastoo, Bitá, Pegah, Ramin, Morteza, Houman, Abbas, Sadegh, Abolfazl, Ebrahim, Behrooz, Navid, and Sarmad for making me feel at home.

Last but not least, my outmost gratitude goes to my precious family, especially my parents and my brother, for your support and encouragement in all steps of my life. Finally, I would like to finish with a Persian poem, reminding me some good memories:

زندگی صحنه‌ی یکتای هنرمندی ماست  
هرکسی نغمه خود خواند و از صحنه رود  
صحنه پیوسته به جا است...

خرم آن نغمه که مردم بسازند به یاد

ژاله اصفهانی

Translation: Life is a unique artistry scene, everybody sings his/her own song and finally leaves the scene, but the scene is always there..., the prosperous song is the one that people remember (Zhale Esfahani).

Alireza Sheikh

Gothenburg, August 2017

# Acronyms

AIR	Achievable Information Rate
ASE	Amplified Spontaneous Emission
AWGN	Additive White Gaussian Noise
BCH	Bose-Chaudhuri-Hocquenghem
BDD	Bounded Distance Decoding
BICM	Bit-Interleaved Coded Modulation
CD	Chromatic Dispersion
CM	Coded Modulation
DAC	Digital-to-Analog Converter
DBP	Digital Back Propagation
DE	Density Evolution
DMC	Discrete Memoryless Channel
DRFA	Distributed Raman Fiber Amplifiers
DS	Direct Sampling
DSP	Digital Signal Processing
EDFA	Erbium-Doped Fiber Amplifier
FEC	Forward Error Correction
FIR	Finite Impulse Response
FOC	Fiber Optical Channel
GVD	Group Velocity Dispersion
HdChaD	Hard detection Channel aware Decoding
HdChaD-BW	Bit-Wise Hard detection Channel aware Decoding
HdChaD-SW	Symbol-Wise Hard detection Channel aware Decoding
HDD	Hard Decision Decoding
IIR	Infinite Impulse Response
LDPC	Low Density Parity Check
LS-BL	Least Squares Band-Limited
ML	Maximum Likelihood
MZ	Matched Zehnder
NLSE	Nonlinear Schrödinger Equation
Pdf	Probability density function
PMD	Polarization Mode Dispersion
P/S	parallel-to-serial
QSC	Q-ary Symmetric Channel
RS	Reed Solomon
RV	Random Variable
SC-LDPC	Spatially Coupled Low Density Parity Check
SDBP	Stochastic Digital Back Propagation
SDD	Soft Decision Decoding
sHDD	Standard Hard Decision Decoding
sHDD-BW	Bit-Wise Standard Hard Decision Decoding
sHDD-SW	Symbol-Wise Standard Hard Decision Decoding
<sup>x</sup> SMF	Single Mode Fiber
SNR	Signal-to-Noise Ratio
SOP	State-Of-Polarization

# Contents

<b>Abstract</b>	<b>i</b>
<b>Preface</b>	<b>iii</b>
<b>List of Publications</b>	<b>v</b>
<b>Acknowledgments</b>	<b>vii</b>
<b>Acronyms</b>	<b>ix</b>
<b>Contents</b>	<b>xi</b>

## **I Introductory Chapters**

<b>1 Introduction</b>	<b>1</b>
1.1 Organization of the Thesis . . . . .	2
1.2 Notation . . . . .	2
<b>2 Fiber-Optic Communication Systems</b>	<b>3</b>
2.1 Signal Propagation in Fiber-Optic Channels . . . . .	3
2.1.1 Fiber Loss and Amplifier Noise . . . . .	4
2.1.2 Kerr-nonlinearity . . . . .	5
2.1.3 Chromatic Dispersion . . . . .	5
2.1.4 Some other Impairments . . . . .	6
<b>3 Energy-Efficiency in Coherent Fiber-Optic Systems</b>	<b>7</b>
3.1 Components of a Coherent Optical System . . . . .	7
3.1.1 Transmitter . . . . .	7
3.1.2 Optical Link . . . . .	8
3.1.3 Receiver . . . . .	9

<b>4</b>	<b>CD Compensation Filter and Code Design for Energy-Efficient Coherent Optical Systems</b>	<b>11</b>
4.1	CD Compensation Filter Design . . . . .	11
4.2	AIRs for CM with Hard Decision Decoding . . . . .	13
4.2.1	Staircase Codes . . . . .	15
4.2.2	Density Evolution . . . . .	16
<b>5</b>	<b>Contributions and Future Work</b>	<b>19</b>
5.1	Paper A . . . . .	19
5.2	Paper B . . . . .	19
5.3	Paper C . . . . .	20
5.4	Future Work . . . . .	20

## II Included Papers

<b>Paper A</b>	<b>Dispersion Compensation FIR Filter with Improved Robustness to Coefficient Quantization Errors</b>	<b>33</b>
1	Introduction . . . . .	33
2	Preliminaries . . . . .	35
2.1	Motivation for a New Filter Design . . . . .	36
3	Proposed FIR CD compensation filter design . . . . .	37
3.1	Filter tap calculations . . . . .	39
3.2	Threshold selection . . . . .	40
4	Simulation Results . . . . .	42
5	Conclusion . . . . .	48
6	Appendix I: Proof of Theorem 1 . . . . .	48
	References . . . . .	52

<b>Paper B</b>	<b>Achievable Information Rates for Coded Modulation with Hard Decision Decoding for Coherent Fiber-Optic Systems</b>	<b>55</b>
1	Introduction . . . . .	55
2	Preliminaries . . . . .	57
2.1	Coded Modulation with Symbol-Wise Soft Decision Decoding	58
2.2	Coded Modulation with Symbol-Wise Hard-Detection Channel-Aware Decoding . . . . .	58
2.3	Coded Modulation with Symbol-Wise Standard Hard Decision Decoding . . . . .	59
3	Achievable Information Rates for Symbol-Wise Decoding and Uniform Input Distribution . . . . .	59
3.1	Achievable Information Rate for Symbol-Wise Soft Decision Decoding . . . . .	60

3.2	Achievable Information Rate for Symbol-Wise Hard Detection Channel-Aware Decoding . . . . .	60
3.3	Achievable Information Rate for Symbol-wise Standard Hard Decision Decoding . . . . .	60
4	Achievable Information Rates with Bit-Wise Decoding . . . . .	62
5	Numerical Results . . . . .	63
5.1	Achievable Information Rates for the AWGN channel . . . . .	63
5.2	Achievable Information Rates for the Fiber-Optic Channel . . . . .	67
6	Conclusion . . . . .	69
7	Density Evolution for Nonbinary GLDPC/SC-GLDPC Codes . . . . .	70
	References . . . . .	76
 <b>Paper C Nonbinary Staircase Codes for Spectrally and Energy Efficient Fiber-Optic Systems</b>		<b>79</b>
1	Introduction . . . . .	79
2	Nonbinary Staircase Codes . . . . .	80
3	Density evolution . . . . .	80
4	Results and Discussion . . . . .	83
5	Conclusion . . . . .	84
6	Acknowledgment . . . . .	84
	References . . . . .	85





# Part I

## Introductory Chapters



# Introduction

Probably most of the people who use their cell phones daily, send emails, chat with their friends via different applications, watch movies online, and use social media networks, do not recognize that in a way, their messages are transformed into photons somewhere and transmitted through fiber-optic links. Optical fibers are used as the Internet backbone and to a less extent as the backhaul network in wireless communications. The communication distance in optical systems varies from few meters in data centers to thousands of kilometers for transoceanic links. Compared to wireless communication, optical communication has the benefit of unlicensed transmission without electromagnetic interference. For transmission over long distances with high aggregated data rates, optical communication is the most prevalent communication method since optical fibers yield substantially lower loss compared to other communication mediums.

Traditionally, optical communication was based on on-off keying modulation at the transmitter and power detection at the receiver. The advent of erbium-doped fiber amplifiers (EDFAs) along with lasers with narrow line-width enabled the emergence of coherent optical communications. These technical developments boosted the data rates from 1 Gb/s in the mid-1980 to 1 Tb/s in 2000 [1]. Coherent optical systems increase the spectral efficiency since the data can be modulated in both the in-phase and quadrature components of the optical field. The spectral efficiency can be increased further by using two polarizations jointly, taking the interaction between polarizations into account using digital signal processing (DSP) at the receiver.

In fiber-optic communications, several impairments, such as chromatic dispersion (CD), fiber loss, nonlinearity, and polarization mode dispersion (PMD), deteriorate the transmitted signal. These impairments must be compensated for in the DSP block of the receiver. To cope with the increasing demand for network capacity, higher data rates are needed, meaning that sophisticated algorithms should be deployed in the DSP of the receiver. In particular, DSP algorithms such as digital back propagation (DBP) [2] and stochastic DBP (SDBP) [3] have been proposed. While using these

algorithms results in compensating fiber impairments to a large extent, it increases the complexity of the receiver, which in turn increases the energy consumption. In 2010, the electric power consumption due to Internet usage was approximately 5% of the worldwide production. With traffic doubling every 18 months, around 2018 the Internet would use twice the electricity generated in 2010 [4]. This motivates the improvement of the energy consumption of point-to-point coherent fiber-optic systems, which are used to handle the Internet traffic. In this thesis, we tackle the energy efficiency of point-to-point fiber-optic communication systems from an algorithmic perspective.

## 1.1 Organization of the Thesis

This thesis is a technical report to support the fulfillment of the requirements for the licentiate degree, a predoctoral degree in the process towards the Ph.D. degree in Sweden, which is formally written in the third year of the Ph.D. candidate. The thesis is divided in two parts. The first part serves as an introduction and gives some background to ease understanding of the second part. The second part consists of appended papers.

The rest of the thesis is organized as follows. In Chapter 2, we briefly discuss signal propagation across the fiber and the main impairments. Chapter 3 discusses the major energy consuming components of a coherent system, which motivates our approach in filter and code design to improve the energy efficiency of coherent systems, presented in Chapter 4. Finally, Chapter 5 serves as a brief description of Part II, which contains the appended papers.

## 1.2 Notation

The following notation is used throughout the thesis. We denote by  $p_X(\cdot)$  the probability mass function (pmf) or the probability density function (pdf) of a (discrete or continuous) random variable (RV)  $X$ .  $P_{\hat{X}|X}(\hat{X}|X)$  denotes the pdf of the RV  $\hat{X}$  on condition  $X$ . We use boldface letters to denote vectors and matrices, e.g.,  $\mathbf{x}$  and  $\mathbf{X}$ , respectively. Expectation with respect to the pmf or pdf of RV  $X$  is denoted by  $\mathbb{E}_X(\cdot)$ .  $(\cdot)^\top$  and  $(\cdot)^H$  stand for the transpose and hermitian conjugate operations, respectively.  $|\cdot|$  gives the absolute value while  $\lfloor \cdot \rfloor$  gives the nearest integer value less than the input value. Furthermore, calligraphic letters are used for sets.

# Fiber-Optic Communication Systems

The optical fiber consists of a cylindrical core made of silica glass that is surrounded by a cladding layer. The cladding layer has a lower refractive index than the fiber core, which leads to guiding the light along the main axis of the fiber. This phenomenon is called *internal reflection* [5]. The propagation of the light inside the fiber can be examined by solving Maxwell's equations. Each solution of Maxwell's equations satisfying the boundary conditions of the fiber is called a *propagation mode* of the fiber. Fibers with more than one mode are used for noncoherent transmission and short distance applications such as transmission in data centers. On the contrary, single mode fibers (SMF) have only one propagation mode, known as the *fundamental mode*, and are used mainly in long-haul coherent optical systems. Although SMFs provide much lower loss compared to copper wires, enabling the extension of the transmission reach, amplifiers are yet required for transmission over long distances. Amplifiers add noise to the original signal, leading to the so-called *signal-noise interaction* phenomenon during propagation. Optical fiber impairments such as group velocity dispersion and Kerr-nonlinearity also distort the transmitted signal. In this thesis, we consider SMFs. In the rest of this chapter, without going into the mathematical details, we will briefly describe the light propagation inside the fiber and the major impairments.

## 2.1 Signal Propagation in Fiber-Optic Channels

The optical fiber is divided into 80-120 km segments where each segment is equipped with an optical amplifier to compensate for the span loss (see Fig. 2.1). Propagation of a single-polarized ( $X$ -polarization) signal over a fiber-optic channel can be described by the nonlinear Schrödinger equation (NLSE),

$$\frac{\partial E_x(t, z)}{\partial z} - i\gamma |E_x(t, z)|^2 E_x(t, z) + i\frac{\beta_2}{2} \frac{\partial^2 E_x(t, z)}{\partial t^2} + \frac{\alpha}{2} E_x(t, z) = 0, \quad (2.1)$$

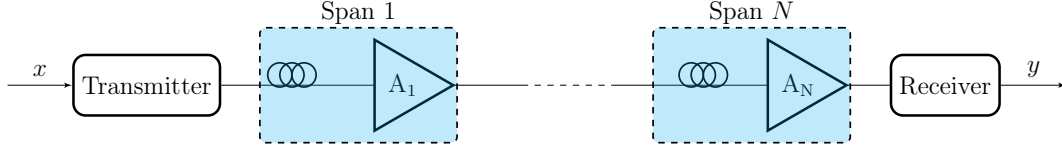


Figure 2.1: A fiber-optic link with  $N$  spans, input  $x$ , and output  $y$ . Each span consists of an amplifier.

where  $E_x(t, z)$  is the envelope of the optical field,  $\gamma$  is the nonlinear coefficient,  $\beta_2$  is the group velocity dispersion parameter,  $\alpha$  is the loss parameter,  $z$  is the propagation distance, and  $t$  is the time coordinate moving with a speed corresponding to the group velocity of the signal. One can increase the spectral efficiency of the system by transmitting a signal in the “Y-polarization”, simultaneously. Propagation over two polarizations implies that interactions between polarizations should be taken into account. Since the polarization state changes rapidly, it can be shown that the propagation of different polarizations averaged over fast changing polarization states can be described by the Manakov equation [6, 7],

$$\frac{\partial \mathbf{E}(t, z)}{\partial z} - i\gamma \frac{8}{9} \|\mathbf{E}(t, z)\|^2 \mathbf{E}(t, z) + i\frac{\beta_2}{2} \frac{\partial^2 \mathbf{E}(t, z)}{\partial t^2} + \frac{\alpha}{2} \mathbf{E}(t, z) = 0, \quad (2.2)$$

where  $\mathbf{E} \triangleq [E_x, E_y]^T$  is a vector containing the field envelopes in two polarizations, and  $\|\mathbf{E}(t, z)\|^2 \triangleq \mathbf{E}^H \mathbf{E}$ . One can see (2.2) as two coupled equations for the two polarizations. In the following, we explain different fiber impairments, described by both Schrödinger and Manakov equations, in more detail.

### 2.1.1 Fiber Loss and Amplifier Noise

If we neglect the dispersion and nonlinearity, i.e.,  $\beta_2 = \gamma = 0$ , the Manakov equation has the closed-form solution

$$\mathbf{E}(t, z) = \mathbf{E}(t, 0) \exp(-\alpha z/2). \quad (2.3)$$

Therefore, the propagated signal in the fiber experiences an exponential decay due to the fiber loss. Silica fibers exhibit wavelength-dependent fiber loss with minimum loss around 1550 nm, which corresponds to 0.2 dB/km. Thus, the center frequency of optical systems is usually set to 1550 nm. Due to the fiber loss, after a certain fiber length, it is required to amplify the signal in order to transmit over larger distances. The use of optical amplifiers in long-haul systems became widespread in the 1990s and by 1996 optical amplifiers were part of the fiber-optic cables laid across the Atlantic and Pacific oceans [5].

Optical amplifiers add noise to the amplified signal, i.e., the signal-to-noise ratio (SNR) of the signal is reduced by the amplifiers. There are two types of optical amplification. In the first type, known as *lumped amplification*, an amplifier boosts the received signal at the end of each span. The signal is amplified

through stimulated emission, which introduces amplified spontaneous emission (ASE) noise. The power spectral density of the ASE noise for each polarization is given by  $G_{\text{ASE}}(\nu) = n_{\text{sp}} h\nu (G - 1)$ , where  $n_{\text{sp}}$  is the spontaneous emission factor,  $h\nu$  is the energy of a photon, and  $G = \exp(\alpha L)$  is the gain of the amplifier for compensating the fiber loss in a span of length  $L$ . In the second type, known as *distributed amplification*, a pump signal transfers its energy to the original signal during propagation through the so-called *stimulated Raman scattering* phenomenon, and the major source of amplifier noise is the spontaneous Raman scattering [7].

### 2.1.2 Kerr-nonlinearity

The Kerr-nonlinearity is due to the fact that the refractive index of the fiber is power dependent. The second term in (2.2) represents the Kerr-nonlinearity effect. In the absence of dispersion, i.e.,  $\beta_2 = 0$ , one can show that the Manakov equation has a closed-form solution given by

$$\mathbf{E}(t, z) = \mathbf{E}(t, 0) \exp(-\alpha z/2) \exp\left(i \frac{8}{9} \gamma L_{\text{eff}}(z) \|\mathbf{E}(t, 0)\|^2\right), \quad (2.4)$$

where  $L_{\text{eff}}(z) = \frac{1 - \exp(-\alpha z)}{\alpha}$  is called the effective length. As can be seen, the nonlinearity can be interpreted as a phase shift in the time-domain response which in turn leads to spectral broadening in the frequency domain, a phenomenon known as *self-phase modulation*. The nonlinear length,  $L_{\text{NL}}$ , is an important parameter and is defined as the fiber length after which the nonlinearity becomes important. For a pulse with peak power  $P_0$  and nonlinear parameter  $\gamma$ , the nonlinear length is  $L_{\text{NL}} = \frac{1}{\gamma P_0}$ . As an example,  $P_0 = -2$  dBm and  $\gamma = 1.3$  (W.km) $^{-1}$  result in  $L_{\text{NL}} = 485$  km.

### 2.1.3 Chromatic Dispersion

In fiber-optic communications, the group velocity is defined as the velocity of the signal envelope. Since the group velocity is frequency dependent, different components of the transmitted signal arrive at different times, which in turn leads to the time-domain broadening of the received signal. This phenomenon is known as *group velocity dispersion* (GVD). To evaluate the effect of dispersion in the Manakov equation, one can neglect loss ( $\alpha = 0$ ) and nonlinearity ( $\gamma = 0$ ) and then find the solution to the Manakov equation as

$$\mathbf{E}(\omega, z) = \mathbf{E}(\omega, 0) \exp\left(i \omega^2 \frac{\beta_2}{2} z\right). \quad (2.5)$$

The GVD can also be expressed based on the dispersion parameter, defined as  $D = -\frac{2\pi c \beta_2}{\lambda^2}$ . In fact, the effect of GVD can be seen as a filter with frequency response

$$H_{\text{CD}}(\omega) = \exp\left(-i \frac{D \lambda^2 z}{4\pi c} \omega^2\right). \quad (2.6)$$

As can be seen, the dispersion behaves as an all-pass filter in the frequency domain with a phase with quadratic frequency dependency. The phase in the frequency domain results in pulse broadening in time domain which, in turn, leads to inter-symbol interference (ISI). The dispersion length is defined as  $L_D = \frac{1}{|\beta_2|w^2}$ , where  $w$  is the signal bandwidth.  $L_D$  indicates the approximate fiber length after which the dispersion becomes important, e.g., for  $D = 17$  ps/nm/km and  $w = 32$  GHz,  $L_D=45$  km.

Chromatic dispersion can be compensated for in the optical domain, using dispersion compensating fibers, or in the digital domain, using DSP at the receiver. In order to compensate the dispersion optically, each span is connected to a short length fiber having a dispersion parameter with opposite sign to that of the dispersion parameter of the underlying fiber. In coherent fiber-optic systems, the dispersion is compensated in the digital domain using DSP. In this case, one can compensate the CD using a finite impulse response (FIR) filter or an infinite impulse response (IIR) filter in the time domain. Another approach is to compensate the CD in the frequency domain using the overlap-save method [8]. In long-haul coherent optical communication, CD is usually compensated in the frequency domain since the number of time-domain filter taps becomes large and the complexity of the implementation increases. On the contrary, recent studies confirm that it is beneficial from a complexity and energy consumption perspectives to use the time-domain CD compensation for short length links [8].

### 2.1.4 Some other Impairments

Communication over the fiber-optic channel comes with some other impairments such as PMD and state-of-polarization (SOP) drifts. PMD results from the fact that the light travels with different speeds for different polarizations, leading to differential group delay between two polarizations. In order to demultiplex the polarization-multiplexed signal, one needs to know the SOP, which may slowly drift with time in a random fashion. This phenomenon is known as the *SOP drift*. In this thesis we neglect these impairments, i.e., we assume that the SOP is perfectly tracked and that the light travels with the same speed for both polarizations.



## Energy-Efficiency in Coherent Fiber-Optic Systems

Coherent fiber-optic communication systems provide higher spectral efficiencies compared to non-coherent systems since data can be transmitted and detected in both the in-phase and quadrature components. Furthermore, coherent transmission enables using sophisticated DSP methods to improve the system performance which in turn leads to increasing the transmission reach. However, using more complex algorithms in the DSP results in an increased energy consumption. Several studies have addressed the estimation of the energy consumption of coherent optical systems and several implementations have been proposed [9–13]. In the following, first we briefly explain the main components of a coherent optical system and then we compare the overall energy consumption in a special case study.

### 3.1 Components of a Coherent Optical System

#### 3.1.1 Transmitter

The transmitter (see Fig. 3.1) consists of different components. The main components are the laser, encoder, pulse shaping, parallel-to-serial converter (P/S), digital-to-analog converter (DAC), and the modulator. The laser provides the carrier and its energy consumption depends on the technology under consideration. The energy consumption of the encoder depends on the code used. For long-haul systems, codes on graphs like low-density parity-check (LDPC) codes [14–17] and soft decision decoding (SDD) are used, while for short links algebraic codes such as Reed Solomon (RS) codes and hard decision decoding (HDD) are utilized. More recently, codes such as staircase codes, braided codes and generalized product codes [18–21], which are based on algebraic block codes, and are decoded using HDD, have also been proposed. Codes on graphs decoded using SDD are sometimes referred to as *soft-*

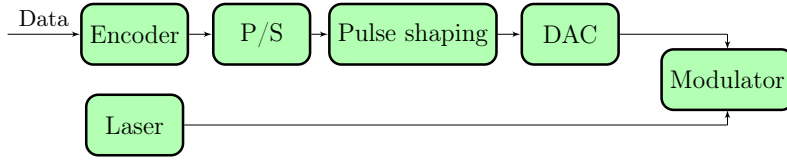


Figure 3.1: The components of the transmitter of a coherent fiber-optic system.



Figure 3.2: The components of the DSP of a coherent fiber-optic system.

*decision* forward error correction (FEC) in the optical communications jargon, while codes decoded using HDD are often referred to as hard-decision FEC. A discussion on different codes is given in Chapter 4.

Soft-decision FEC provides higher net coding gains than hard-decision FEC, but at the expense of a higher energy consumption. The energy consumption of the encoder can be determined by implementing the encoder. Alternatively, it can be roughly estimated by counting the required number of operations for encoding and associating a certain energy consumption to each operation depending on the implementation technology [9]. In general, the encoder can be parallelized in order to reduce the energy consumption. The encoded data is converted to a serial stream which is pulse shaped, and then to an analog signal, used as the input of the matched Zehnder (MZ) modulator. The typical energy consumption of the P/S, DAC, and MZ modulator are summarized in [9, Table I].

### 3.1.2 Optical Link

The energy consumption of the optical link is mainly due to the energy consumption of the amplifiers. In [22], the energy consumption of the EDFAs and distributed Raman fiber amplifiers (DRFAs) is estimated based on the required SNR at the receiver. In lumped amplification using EDFAs, the energy consumption of the amplifier depends on the power injected to the fiber and also on a constant term which is known as the monitoring and management energy consumption ( $P_{mm}$ ).  $P_{mm}$  is due to the required electronics to drive the amplifiers and is the dominant effect in the overall energy consumption of the amplifiers [22–25]. Recently, the authors in [26] proposed a model to estimate the energy consumption of EDFAs and DRFAs. It is shown that for low values of  $P_{mm}$ , the EDFAs are more energy efficient, while for larger values, the DRFAs are preferable for energy-efficient amplification.

### 3.1. COMPONENTS OF A COHERENT OPTICAL SYSTEM

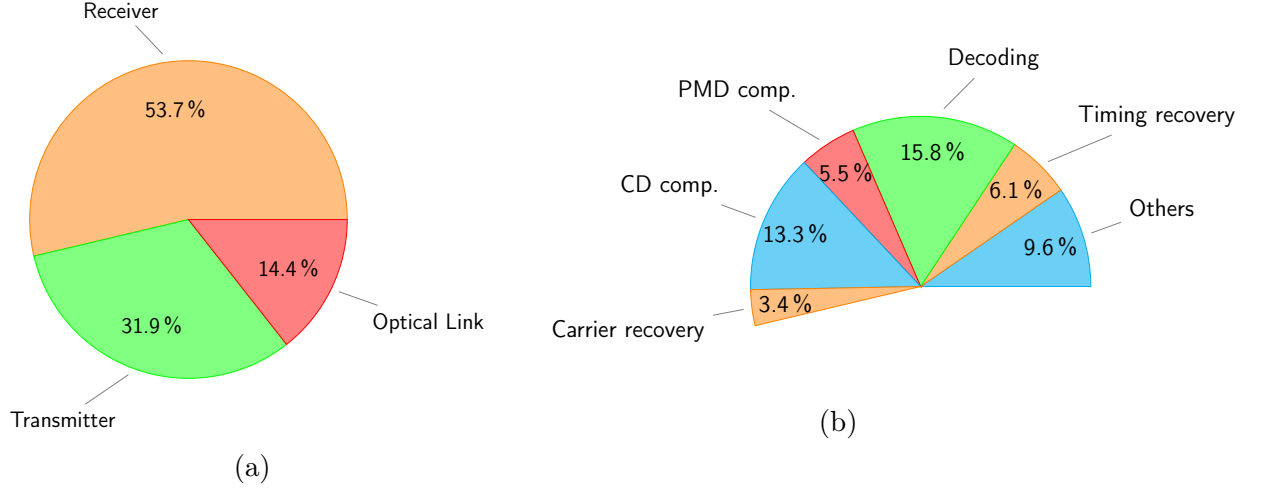


Figure 3.3: (a) The energy consumption of different components of a coherent fiber-optic system for a 2400 km link with lumped amplification and 16-QAM modulation. Data is extracted from [9, Table XVI]. (b) The energy consumption of the receiver components. The numbers give the percentage of the energy consumption out of the overall energy consumption. Data is extracted from [9, Table XVI].

#### 3.1.3 Receiver

The energy consumption of the receiver is mainly dominated by the energy consumption of the DSP block [9, 12]. The components of the DSP block are shown in Fig. 3.2. In the CD compensation component, the accumulated CD due to the GVD is compensated for. The energy consumption of the CD compensation depends on the implementation. As shown in [8], for short-haul links such as metro links, time-domain CD compensation implemented using so-called polyphase and fast-FIR structures is more energy efficient compared to the frequency-domain compensation, while for long-haul systems it is beneficial to compensate the CD in the frequency domain. The timing recovery block synchronizes the sampling time at the receiver and can be implemented based on data-aided or blind algorithms [27]. The PMD is usually compensated by an adaptive filter using well-known algorithms such as constant composition or radius directed equalization [28, 29]. The carrier recovery, which is due to the frequency and phase mismatch between the input signal and the local oscillator, is compensated for using the Viterbi-and-Viterbi algorithm [30]. Similar to the encoder, the energy consumption of the decoder highly varies based on the code used and the implementation details. In general, SDD of codes on graphs is significantly more energy-hungry than HDD of algebraic codes such as RS or staircase codes. For this reason, in Papers B and C our focus is on hard-decision FEC.

To have a flavor about the energy consumption of a coherent optical system, we consider a case study presented in [9]. In the case study, the data, of length 20489 bits, is encoded by an LDPC code with code length 24576 bits [14], and transmitted over a 2400 km link with lumped amplification using 16-QAM. Fig. 3.3(a) summarizes the

portion of the overall energy consumption corresponding to the transmitter, optical amplifiers, and the receiver. As can be seen, the receiver is the most energy-hungry. In Fig. 3.3(b), the energy consumption of the different components of the receiver is shown. One can see that the CD compensation and the decoder are the major energy-hungry blocks. This motivates the design of a new, energy efficient CD compensation filter in Paper A and the analysis of achievable information rates (AIRs) for HDD and the design of hard-decision FEC in Papers B and C.

# CD Compensation Filter and Code Design for Energy-Efficient Coherent Optical Systems

In this chapter, we briefly motivate and discuss the proposed CD compensation filter and code design for energy-efficient coherent optical systems.

## 4.1 CD Compensation Filter Design

According to (2.6), the frequency response of the CD compensation is an all-pass filter,

$$H_{\text{CD}}^{-1}(\omega) = \exp\left(i \frac{D\lambda^2 z}{4\pi c} \omega^2\right), \quad (4.1)$$

where  $c$  is the speed of light and  $\lambda$  is the wavelength. One can design an FIR or IIR filter with the frequency response (4.1). Due to the inherent instability of IIR filters, FIR filters are of interest for CD compensation [31,32]. The FIR filter can be used as a component of frequency-domain compensation algorithms such as the overlap-and-save method, or it can be used directly in time-domain CD compensation. In [31], an FIR CD compensation filter, given in closed form, was proposed by performing direct sampling (DS) and truncation of the ideal CD compensation impulse response.

The DS filter compensates the CD in the whole frequency band, while in a practical system the transmitted signal is band limited due to pulse shaping. Thus, the filter attempts to compensate the CD even in the frequency band without signal content. Therefore, potentially, one can reduce the number of filter taps and compensate the same accumulated CD by a better filter design. In [32], the authors proposed a new filter which takes into account the effect of pulse shaping at the transmitter.

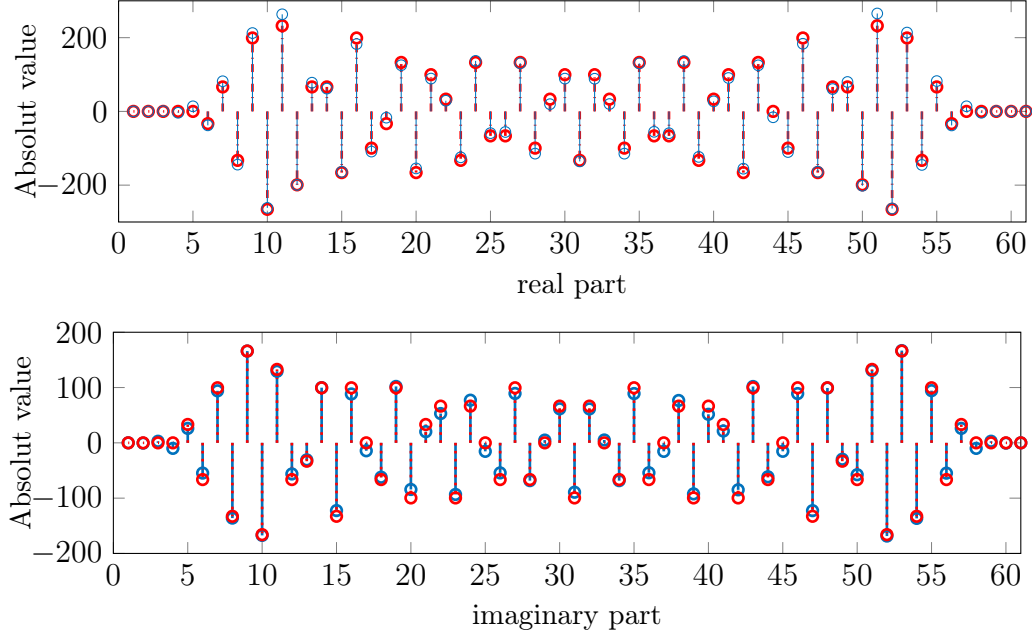


Figure 4.1: The real and imaginary parts of the filter coefficients of the LS-BL filter with 61 taps with floating point precision (blue) and quantized filter with 4-bit word length (red).

The proposed filter is based on a least-squares optimization problem given as

$$\tilde{\mathbf{h}} = \arg \min_{\mathbf{h}} \xi_s, \quad (4.2)$$

where  $\mathbf{h} = [h_{-(N-1)/2}, \dots, h_0, \dots, h_{(N-1)/2}]^T$  is the filter tap coefficient vector and  $\xi_s$  is the in-band error defined as the error between the frequency response of the ideal CD compensation filter and the frequency response of the FIR filter with coefficients  $\mathbf{h}$  (see [32, Eg. 6]). For the ease of exposure, we refer to this filter as the least-squares band-limited (LS-BL) filter. As shown in [32], the LS-BL filter achieves the same performance as that of the DS filter with approximately 50% fewer number of filter taps. Since reducing the number of taps results in decreasing the implementation complexity and energy consumption accordingly, the LS-BL filter is a candidate for energy-efficient CD compensation.

The works [31,32] implicitly assume that filter taps are implemented with floating-point precision. In practice, however, filter taps must be implemented in finite precision. Coefficient quantization distorts the values of the coefficients, leading to quantization errors which, in turn, change the frequency response of the designed filter. As an example, consider the LS-BL filter with 61 taps, root-raised cosine pulse shaping and fiber parameters given in [33, Table I]. In Fig. 4.1, the real and imaginary parts of the filter tap coefficients of the LS-BL filter with floating point precision and the quantized filter using linear quantization [33, Sec. III.B] with 4-bit word length are shown. As can be seen, quantization alters the real and imaginary parts of the filter taps, which in turn changes both the amplitude and phase response of the

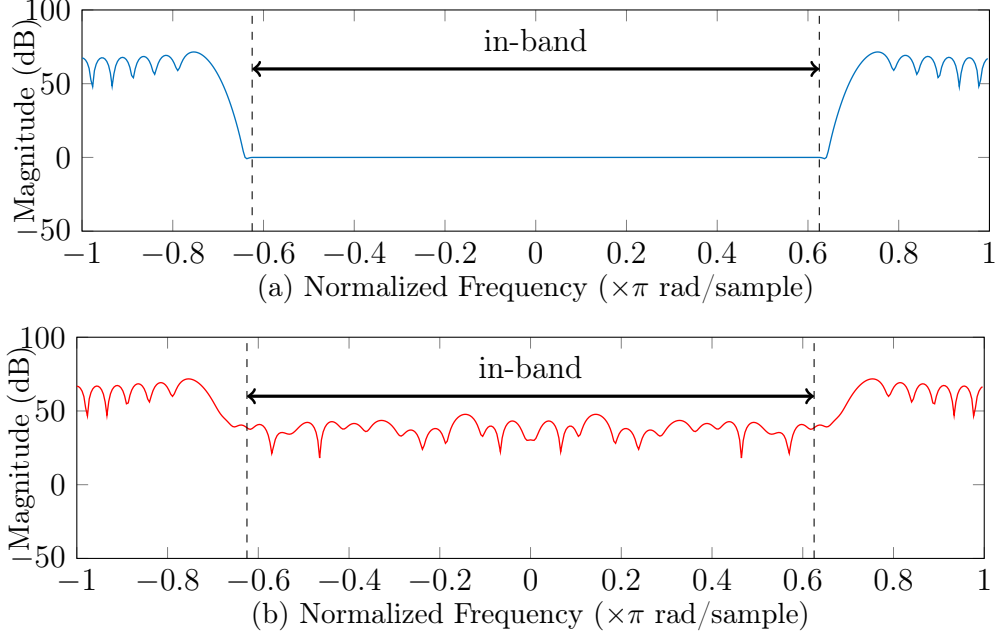


Figure 4.2: Amplitude response of the LS-BL filter with 61 taps and floating point precision (blue curve) and corresponding fixed-point filter using 4-bit word length (red curve).

underlying filter. Fig. 4.2 depicts the amplitude response of the LS-BL filter shown in Fig. 4.1. We remark that in Fig. 4.2 the in-band frequencies are  $[-0.625\pi, 0.625\pi]$ . It can be observed that the LS-BL filter with floating point precision provides the desired all-pass amplitude response while the in-band response of the quantized filter is significantly distorted. In fact, a high quantization error translates into a lot of distortion in the frequency domain. Therefore, it is required to incorporate the effect of quantization errors in the filter design, especially with respect to energy efficiency considerations, where the number of filter taps should be reduced as low as possible. This observation motivates the design in Paper A of an FIR filter with improved robustness to coefficient quantization errors.

## 4.2 AIRs for CM with Hard Decision Decoding

Coded modulation (CM) is a technique to improve the spectral efficiency while delivering the data reliably. In a CM system, one can use binary or nonbinary codes at the transmitter and SDD or HDD at the receiver. This gives rise to four different types of CM: bit-wise SDD, bit-wise HDD, symbol-wise SDD, and symbol-wise HDD. LDPC codes [14, 34] and spatially-coupled LDPC (SC-LDPC) codes [35, 36] with SDD provide large coding gains, but at the cost of high decoding complexity and data flow at the decoder. An alternative is to use algebraic codes and HDD, which significantly reduces the decoding complexity and data flow, which translate in a significantly

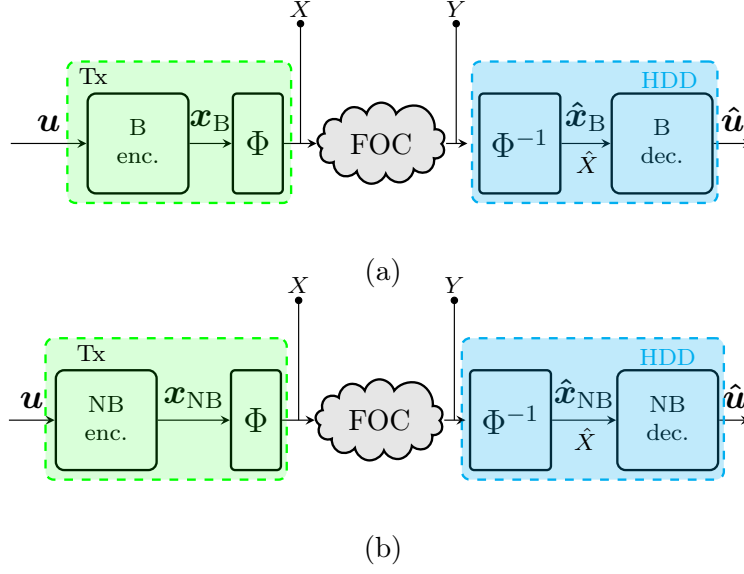


Figure 4.3: System model of the CM using binary (B) and nonbinary (NB) codes and HDD.

lower energy consumption. Hence, there is an interest in using codes with HDD for energy-efficient optical systems. In particular, binary staircase codes [18, 19], braided codes [20], and generalized product codes [21] yield very large coding gains yet with low decoding complexity. These codes are decoded using iterative bounded distance decoding (BDD), which is based on the Berlekamp-Massey algorithm [37, 38] and uses the Hamming distance metric.

In this thesis, due to energy consumption considerations, we consider HDD. In Fig. 4.3, the block diagram of a CM scheme with HDD for both binary and nonbinary encoding/decoding is shown. In Fig. 4.3(a), for binary transmission, the data sequence  $\mathbf{u}$  is encoded to codeword  $\mathbf{x}_B$  using a binary code. The code bits  $x_B^i$  are mapped to the symbols of a constellation by the mapper  $\Phi$  using the bit-interleaved coded modulation (BICM) paradigm. Alternatively, a nonbinary code matched to the constellation size can be used, as shown in Fig. 4.3(b). In this case, the code sequence  $\mathbf{x}_{NB}$  is a sequence of nonbinary symbols, which are mapped to the constellation symbols. The sequence of modulated symbols is then transmitted over the fiber-optic channel (FOC).

At the receiver, for symbol-wise decoding, the received symbol  $y_i$  is hard detected to  $\hat{x}_i$  using  $\Phi^{-1}$  as

$$\hat{x}_i = \arg \max_{x \in \mathcal{X}} p_{Y|X}(y_i|x), \quad (4.3)$$

where  $\mathcal{X}$  is the set containing the symbols of the constellation, of order  $M$ , and  $\hat{\mathbf{x}}_{NB} = (\hat{x}_1, \hat{x}_2, \dots)$ . For bit-wise decoding, we also consider that the received symbol  $y_i$  is hard detected according to (4.3). Then,  $\hat{\mathbf{x}}_B = (b(\hat{x}_1), b(\hat{x}_2), \dots)$ , where  $b(\hat{x}_i)$  is a vector of  $m$  bits corresponding to the binary image of  $\hat{x}_i$ .

A useful parameter to determine the ultimate performance limits of CM schemes



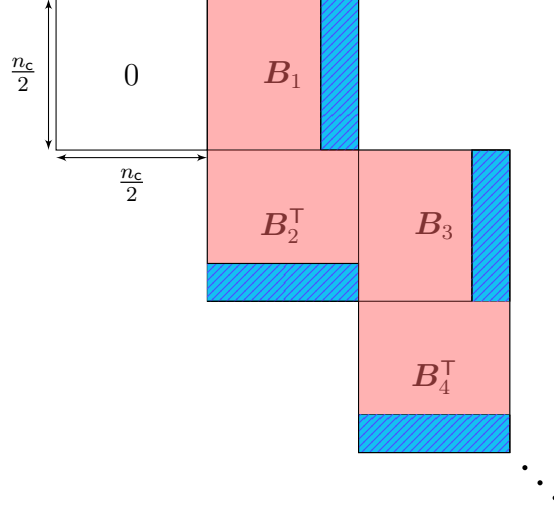


Figure 4.4: The code array of a staircase code. Information bits and parity bits are shown with red and blue hatches, respectively.

and compare them, is the AIR, which provides a lower bound on the mutual information of the system, i.e., the maximum rate at which reliable communication is possible. To the best of our knowledge, surprisingly, AIRs for CM with HDD have not been considered in the literature. Only the paper [39] considered AIRs for what the authors called a “HDD”. However, [39] implicitly assumes that the decoder makes use of the channel transition probabilities of the discrete memoryless channel (DMC) resulting from the hard detection. As such, this decoder cannot be considered a hard decision decoder, which is based on the Hamming distance metric [40–44]. Therefore, in Paper B we analyze AIRs for HDD with bit-wise and symbol-wise decoding.

### 4.2.1 Staircase Codes

In this thesis, we consider staircase codes as a powerful hard-FEC scheme. Binary staircase codes with Bose-Chaudhuri-Hocquenghem (BCH) component codes, proposed by Smith *et al.* [18], provide large net coding gains. The staircase code in [18] with roughly 7% overhead provides 0.42 dB net coding gain improvement compared to the best proposed code from the ITU-T G.975.1 recommendation at bit error rate  $10^{-15}$ . The impressive performance of staircase codes, together with their low complexity algebraic decoding, makes them an interesting option for future fiber-optic systems.

A staircase codes is defined by a two-dimensional array that has the form of a staircase. The code array is shown in Fig. 4.4. The structure of the staircase code imposes that each code bit is protected by two component codes, a row code and a column code. For the encoding, the first block of the code array is initialized with zeros. Information bits are then placed in the first part of the second block (shown

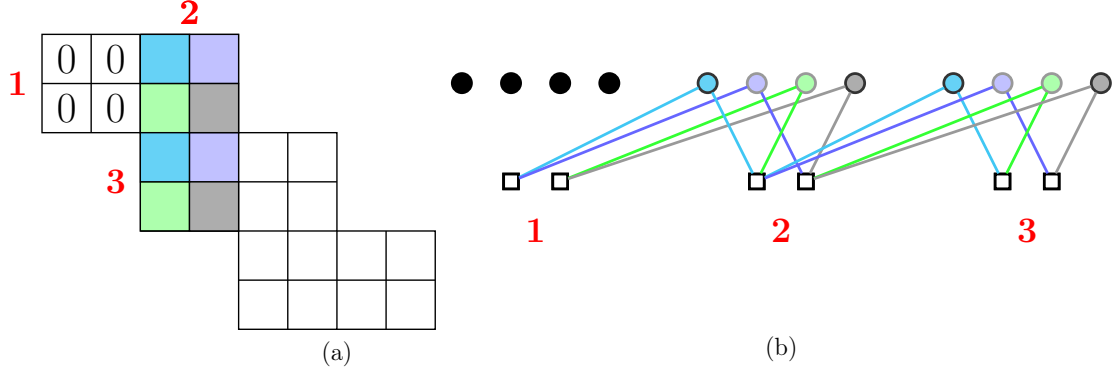


Figure 4.5: (a) An example of a staircase code with 4 coded symbols per each spatial position, and (b) the corresponding bipartite graph.

with red color in Fig. 4.4), which can be represented by a binary matrix  $\mathbf{B}_1$ . By row encoding, parity bits (shown with blue hatches) are generated. Then, data bits are placed in the first part of the third block, represented by a binary matrix  $\mathbf{B}_2$  (see Fig. 4.4), and column encoding is performed. This procedure continues for encoding the next blocks. In particular, each row of  $[\mathbf{B}_{i-1}^T, \mathbf{B}_i]$  is a valid codeword of the BCH component code.

Staircase codes are decoded using iterative BDD. BDD corrects all error patterns with Hamming weight up to the error-correcting capability of the code. In particular, decoding is performed in a window-decoding fashion, i.e., the decoder iterates between row and column decoding for the blocks inside a given window for a predefined number of iterations. The size of the window provides a tradeoff between performance and decoding latency, i.e., one expects a performance improvement by increasing the window size at the expense of a higher decoding latency.

In Paper C, we consider the design of nonbinary staircase codes.

## 4.2.2 Density Evolution

Density evolution (DE) is a mathematical tool to estimate the asymptotic performance of codes on graphs. More precisely, the DE allows to predict the iterative decoding threshold of a code ensemble, i.e., the channel parameter for which the probability of error goes to zero under belief propagation decoding (as the block length goes to infinity). In coding theory, determining the iterative decoding threshold for a particular (deterministic) code is very difficult. In contrast, analyzing code ensembles is much easier. One can use the DE analysis to optimize code parameters so that the iterative decoding threshold is optimized.

Staircase codes can be seen as a class of SC-GLDPC codes [19]. In Fig. 4.5(a), we depict the code array of a staircase code with 4 code symbols per block and the corresponding bipartite graph. In the bipartite graph, each staircase block corresponds to one spatial position. As an example, the first three blocks and spatial

positions are numbered in Fig. 4.5. In the bipartite graph, the variable nodes (VNs), represented by circles, correspond to code symbols, while the constraint nodes (CNs), represented by squares, correspond to the row and column codes. For instance, the squares in spatial position 1 correspond to the first two row codes while the squares in spatial position 2 correspond to the first two column codes. An edge is drawn between a VN and a CN if the corresponding code bit participates in the corresponding row/column code. In the figure, the code symbols and the corresponding edges for spatial positions 2 and 3 are shown with the same color, e.g., in Fig. 4.5(b), the first code symbol in spatial position 2 (shown in blue), is connected to the first component code in spatial positions 1 and 2. As can be seen, each code symbol in spatial position  $i$  is connected to one component code in spatial position  $i$  and one component code in the spatial position  $i - 1$ . From Fig. 4.5, one can readily infer that the staircase code is contained in the ensemble of SC-GLDPC codes with coupling width 2 [19].

In [20], the DE for binary SC-GLDPC codes with BCH component codes was derived. In [19], by observing that staircase codes are contained in the SC-GLDPC ensemble in [20], the parameters of staircase codes were optimized using DE to optimize the iterative decoding threshold. This approach dramatically decreases the optimization time compared to a simulation-based approach. In Paper B, we extend the DE analysis in [20] to nonbinary SC-GLDPC codes with RS component codes. Then, in Paper C we use the derived DE to design the parameters of nonbinary staircase codes with RS component codes.



## Contributions and Future Work

### 5.1 Paper A

In Paper A, we design an FIR filter with increased robustness to coefficient quantization errors compared to the existing filters in the literature. We motivate the use of FIR filters for time-domain CD compensation in the low-to-moderate accumulated CD regime such as transmission in metro links. Existing filter design methods implicitly assume a floating point implementation, i.e., quantization errors due to a finite word length are neglected. We show that some of the existing filters perform significantly different in the presence of quantization errors and cannot be used in practice. We identify a relation between the out-of-band gain of the filter and quantization errors and also a tradeoff between quantization errors and in-band errors. In particular, we find that a large out-of-band gain increases the quantization error while reduces the in-band error. Therefore, we propose a new filter design, given in closed-form, based on a constrained least-squares optimization problem to minimize the in-band error while confining the out-of-band gain. Simulation results confirm that for a given coefficient quantization word length, the proposed filter outperforms the existing filters in the literature.

### 5.2 Paper B

In Paper B, we analyze the AIRs for CM with HDD. In particular, we assume the standard HDD where decoding is based on the Hamming distance metric [40–44]. This is the HDD widely used in practice to decode BCH codes and RS codes, as well as product codes and their generalizations. AIRs for CM have been recently analyzed in [39]. However, the decoder referred to as “HDD” in [39] exploits the channel transition probabilities of the DMC resulting from the hard detection of the channel output. As such, the “HDD decoder” in [39] exploits soft information and

therefore does not fall within the standard definition of HDD. Furthermore, this is not the HDD used in practice and it is not clear how it can be implemented with low complexity.

In Paper B, we therefore derive the AIRs for the standard HDD based on the Hamming distance metric for both bit-wise and symbol-wise decoding, corresponding to the use of binary codes (using the BICM paradigm) and nonbinary codes, respectively. An important outcome of this paper is that the AIRs of bit-wise decoders are significantly larger than those of symbol-wise decoders. Therefore, for HDD binary codes are to be preferred for high spectrally efficient fiber-optic communications. This is in sharp contrast with the conclusion in [39], where it was shown that for the decoder that exploits the channel transition probabilities of the DMC, symbol-wise decoding yields higher AIRs. The conclusion arising from our AIRs analysis is confirmed by performance results of binary and nonbinary staircase codes. For nonbinary staircase codes, we derive the DE analysis of the underlying SC-GLDPC code ensemble and optimize the RS code components based on the DE.

### 5.3 Paper C

In Paper C, we design nonbinary staircase codes with RS codes as component codes. In particular, we consider nonbinary staircase codes as a particular instance of (non-binary) SC-GLDPC codes. For decoding, we consider the standard HDD of staircase codes, i.e., iterative BDD based on the Hamming distance metric. We consider the additive white Gaussian noise (AWGN) channel as a proxy of the fiber-optic channel. With HDD, the AWGN channel (after hard detection) can be modeled as a QSC. We then derive the DE for nonbinary SC-GLDPC codes over the QSC by extending the DE analysis in [20] for SC-GLDPC codes over the binary symmetric channel to the nonbinary case, and optimize the parameters of nonbinary staircase codes based on the DE. By means of simulations, we show that the optimized codes perform best as compared to other nonbinary staircase codes and product codes with the same code rate. The design of nonbinary staircase codes was motivated by the claim in [39] that for HDD symbol-wise decoders achieve larger information rates. However, in Paper B we show that, indeed, for HDD (i.e., the standard and widely used HDD based on the Hamming distance metric) bit-wise decoders yield higher AIRs. The simulation of binary and nonbinary staircase codes in Paper B confirms this conclusion.

### 5.4 Future Work

As can be seen in Fig. 3.3(a), the amplifiers account for a relatively high portion of the overall energy consumption. One can vary the energy consumption of the amplifiers by changing the span length. Essentially, this corresponds to changing the

received SNR, meaning that the considered code (or its code rate) should be changed, which in turn alters the decoder energy consumption. An interesting future work is to evaluate this tradeoff, i.e., finding the optimum span length that minimizes the energy consumption of the amplifiers and the decoder for a given code class and decoding algorithm (e.g., LDPC codes and belief propagation).

In Paper C, for the code design, we assumed the standard HDD based on the Hamming distance metric, which effectively transforms the channel into a QSC. This decoding metric does not necessarily give the highest possible AIR. As shown in [39], if the channel transition probabilities of the DMC resulting from the hard detection of the channel output are exploited, higher AIRs can be obtained. Therefore a question arises: is it possible to modify the decoding metric to incorporate these probabilities without increasing the decoding complexity to that of the SDD? Or, is it possible to devise new decoding metrics (non necessarily exploiting the transition probabilities) that yield to higher AIRs?

We are currently extending the work in Papers B and C by considering probabilistic shaping (see [45, 46]). We have extended the probabilistic amplitude shaping scheme in [47] to HDD and staircase codes and shown significant gains with respect to the baseline scheme using a uniform constellation. An interesting topic for future work is the analysis of the error floor of the probabilistically-shaped CM scheme in [45, 46].





# References

- [1] P. J. Winzer, “Scaling optical fiber networks: Challenges and solutions,” *Optics and Photonics News*, vol. 26, no. 3, pp. 28–35, Mar. 2015.
- [2] E. Ip, “Nonlinear compensation using backpropagation for polarization-multiplexed transmission,” *IEEE/OSA J. Lightw. Technol.*, vol. 28, no. 6, pp. 939–951, Mar. 2010.
- [3] N. V. Irukulapati, H. Wymeersch, P. Johannisson, and E. Agrell, “Stochastic digital backpropagation,” *IEEE Trans. Commun.*, vol. 62, no. 11, pp. 3956–3968, Nov. 2014.
- [4] J. Bowers, “Challenges in silicon as a photonic platform,” Planary talk, in Proc. *Int. Conf. Optical Commun. (ECOC)*, Torino, Italy, 2010.
- [5] G. P. Agrawal, *Fiber-optic communication systems*. New York, NY, USA: John Wiley, 2002.
- [6] A. Napoli, Z. Maalej, V. A. J. M. Sleiffer, M. Kushnerov, D. Rafique, E. Timmers, B. Spinnler, T. Rahman, L. D. Coelho, and N. Hanik, “Reduced complexity digital back-propagation methods for optical communication systems,” *IEEE/OSA J. Lightw. Technol.*, vol. 32, no. 7, pp. 1351–1362, Apr. 2014.
- [7] G. P. Agrawal, *Nonlinear fiber optics*. Waltham, MA, USA: Academic Press, Elsevier, 2002.
- [8] C. Fougstedt, A. Sheikh, P. Johannisson, A. Graell i Amat, and P. Larsson-Edefors, “Power-efficient time-domain dispersion compensation using optimized fir filter implementation,” in *Advanced Photonics*, Boston, MA, 2015, p. SpT3D.3.
- [9] B. S. G. Pillai, B. Sedighi, K. Guan, N. P. Anthapadmanabhan, W. Shieh, K. J. Hinton, and R. S. Tucker, “End-to-end energy modeling and analysis of long-haul

## References

- coherent transmission systems,” *IEEE/OSA J. Lightw. Technol.*, vol. 32, no. 18, pp. 3093–3111, Sep. 2014.
- [10] B. Sedighi, H. Khodakarami, B. S. G. Pillai, and W. Shieh, “Power-efficiency considerations for adaptive long-haul optical transceivers,” *J. Opt. Commun. Netw.*, vol. 6, no. 12, pp. 1093–1103, Dec. 2014.
- [11] L. Lundberg, C. Fougstedt, P. Larsson-Edefors, P. A. Andrekson, and M. Karlsson, “Power consumption of a minimal-DSP coherent link with a polarization multiplexed pilot-tone,” in *Proc. Int. Conf. Optical Commun. (ECOC)*, Düsseldorf, Germany, Sep. 2016, pp. 1–3.
- [12] M. Kuschnerov, T. Bex, and P. Kainzmaier, “Energy efficient digital signal processing,” in *Proc. Optical Fiber Commun. Conf. (OFC)*, San Diego, CA, Mar. 2014, pp. 1–3.
- [13] M. Nazarathy and A. Tolmachev, “Efficient DSP methods for coherent optical receiver,” in *27th Convention of Electrical and Electronics Engineers in Israel*, Israel, Nov. 2012, pp. 1–4.
- [14] D. A. Morero, M. A. Castrillon, F. A. Ramos, T. A. Goette, O. E. Agazzi, and M. R. Hueda, “Non-concatenated FEC codes for ultra-high speed optical transport networks,” in *Proc. IEEE Global Telecommun. Conf. (GLOBECOM)*, Houston, TX, Dec. 2011, pp. 1–5.
- [15] A. Leven and L. Schmalen, “Status and recent advances on forward error correction technologies for lightwave systems,” *IEEE/OSA J. Lightw. Technol.*, vol. 32, no. 16, pp. 2735–2750, Aug. 2014.
- [16] C. Häger, A. Graell i Amat, F. Brännström, A. Alvarado, and E. Agrell, “Terminated and tailbiting spatially coupled codes with optimized bit mappings for spectrally efficient fiber-optical systems,” *IEEE/OSA J. Lightw. Technol.*, vol. 33, no. 7, pp. 1275–1285, Apr. 2015.
- [17] A. Graell i Amat, C. Häger, F. Brännström, and E. Agrell, “Spatially-coupled codes for optical communications: state-of-the-art and open problems,” in *Opto-Electronics and Commun. Conf. (OECC)*, Shanghai, China, Jun. 2015, pp. 1–3.
- [18] B. P. Smith, A. Farhood, A. Hunt, F. R. Kschischang, and J. Lodge, “Staircase codes: FEC for 100 Gb/s OTN,” *J. Lightw. Technol.*, vol. 30, no. 1, pp. 110–117, Jan. 2012.
- [19] C. Häger, A. Graell i Amat, H. D. Pfister, A. Alvarado, F. Brännström, and E. Agrell, “On parameter optimization for staircase codes,” in *Proc. Optical Fiber Commun. Conf. (OFC)*, Los Angeles, CA, 2015, pp. 1–3.

- [20] Y.-Y. Jian, H. D. Pfister, K. R. Narayanan, R. Rao, and R. Mazahreh, "Iterative hard-decision decoding of braided BCH codes for high-speed optical communication," in *Proc. IEEE Global Telecom. Conf. (GLOBECOM)*, Atlanta, GA, Dec. 2013.
- [21] C. Häger, A. Graell i Amat, H. D. Pfister, and F. Brännström, "Density evolution for deterministic generalized product codes with higher-order modulation," in *Proc. 9th Int. Symp. Turbo Codes and Iterative Inf. Processing (ISTC)*, Brest, France, 2016, pp. 236–240.
- [22] P. Wang, K. Hinton, P. M. Farrell, and B. S. G. Pillai, "On EDFA and Raman fiber amplifier energy efficiency," in *Proc. European Conf. Data Science and Data Intensive Systems (DSDIS)*, Sydney, NSW, Australia, Dec. 2015.
- [23] R. S. Tucker, "Green optical communications Part II: Energy limitations in networks," *IEEE J. Select. Topics Quantum Electron.*, vol. 17, no. 2, pp. 261–274, Mar. 2011.
- [24] B. Stiller, T. Bocek, F. Hecht, G. Machado, P. Racz, and M. Waldburger, "Equipment power consumption in optical multilayer networks," Tech. Rep., IBCN-12-001-01, 2012.
- [25] L. Lundberg, P. Johannisson, E. Agrell, M. Karlsson, and P. A. Andrekson, "Power consumption of hybrid EDFA/Raman amplified systems," in *Proc. Int. Conf. Optical Commun. (ECOC)*, Valencia, Spain, Sep. 2015.
- [26] L. Lundberg, P. A. Andrekson, and M. Karlsson, "Power consumption analysis of hybrid EDFA/Raman amplifiers in long-haul transmission systems," *IEEE/OSA J. Lightw. Technol.*, vol. 35, no. 11, pp. 2132–2142, Jun. 2017.
- [27] N. K. Jablon, "Joint blind equalization, carrier recovery and timing recovery for high-order QAM signal constellations," *IEEE Trans. Sig. Processing*, vol. 40, no. 6, pp. 1383–1398, Jun. 1992.
- [28] R. Johnson, P. Schniter, T. J. Endres, J. D. Behm, D. R. Brown, and R. A. Casas, "Blind equalization using the constant modulus criterion: a review," *Proceedings of the IEEE*, vol. 86, no. 10, pp. 1927–1950, Oct. 1998.
- [29] M. J. Ready and R. P. Gooch, "Blind equalization based on radius directed adaptation," in *Int. Conf. Acoustics, Speech, and Signal Processing*, Albuquerque, NM, Apr. 1990, pp. 1699–1702.
- [30] A. Viterbi, "Nonlinear estimation of PSK-modulated carrier phase with application to burst digital transmission," *IEEE Trans. Inf. Theory*, vol. 29, no. 4, pp. 543–551, Jul. 1983.

## References

- [31] S. J. Savory, “Digital filters for coherent optical receivers,” *Opt. Express*, vol. 16, no. 2, pp. 804–817, Jan. 2008.
- [32] A. Eghbali, H. Johansson, O. Gustafsson, and S. J. Savory, “Optimal least-squares FIR digital filters for compensation of chromatic dispersion in digital coherent optical receivers,” *IEEE/OSA J. Lightw. Technol.*, vol. 32, no. 8, pp. 1449–1456, Apr. 2014.
- [33] A. Sheikh, C. Fougstedt, A. Graell i Amat, P. Johannisson, P. Larsson-Edefors, and M. Karlsson, “Dispersion compensation FIR filter with improved robustness to coefficient quantization errors,” *IEEE/OSA J. Lightw. Technol.*, vol. 34, no. 22, pp. 5110–5117, Nov. 2016.
- [34] K. Cushon, P. Larsson-Edefors, and P. Andrekson, “Low-power 400-Gbps soft-decision LDPC FEC for optical transport networks,” *IEEE/OSA J. Lightw. Technol.*, vol. 34, no. 18, pp. 4304–4311, Sep. 2016.
- [35] L. Schmalen, V. Aref, J. Cho, D. Suikat, D. Rösener, and A. Leven, “Spatially coupled soft-decision error correction for future lightwave systems,” *IEEE/OSA J. Lightw. Technol.*, vol. 33, no. 5, pp. 1109–1116, Mar. 2015.
- [36] C. Häger, A. Graell i Amat, F. Brännström, A. Alvarado, and E. Agrell, “Terminated and tailbiting spatially coupled codes with optimized bit mappings for spectrally efficient fiber-optical systems,” *IEEE/OSA J. Lightw. Technol.*, vol. 33, no. 7, pp. 1275–1285, Apr. 2015.
- [37] E. Berlekamp, *Algebraic Coding Theory*. McGraw-Hill, New York, 1968.
- [38] J. Massey, “Shift-register synthesis and bch decoding,” *IEEE Trans. Inf. Theory*, vol. 15, no. 1, pp. 122–127, Jan. 1969.
- [39] G. Liga, A. Alvarado, E. Agrell, and P. Bayvel, “Information rates of next-generation long-haul optical fiber systems using coded modulation,” *IEEE/OSA J. Lightw. Technol.*, vol. 35, no. 1, pp. 113–123, Jan. 2017.
- [40] S. Lin and D. J. Costello Jr., *Error Control Coding, Second Edition*. Upper Saddle River, NJ, USA: Prentice-Hall, Inc., 2004.
- [41] A. Lapidoth, *A foundation in digital communication*. Cambridge, UK: Cambridge University Press, 2009.
- [42] A. Barg, “Complexity issues in coding theory,” *Handbook of Coding Theory*, vol. I, V.S. Pless, W.C. Huffman, Editors, North Holland, 2007.
- [43] V. Guruswami, *List decoding of error-correcting codes*. Springer Science & Business Media, 2004.

## References

- [44] A. Vardy, “Algorithmic complexity in coding theory and the minimum distance problem,” in *Proc. 29th Annual ACM Symp. Theory of Computing*, El Paso, TX, May 1997, pp. 92–109.
- [45] A. Sheikh, A. Graell i Amat, and G. Liva, “Probabilistically-shaped coded modulation with hard decision decoding and staircase codes.” [Online]. Available: <http://arxiv.org/abs/1606.01689>
- [46] —, “Probabilistically-shaped coded modulation with hard decision decoding for coherent optical systems,” in *Proc. Int. Conf. Optical Commun. (ECOC)*, Gothenburg, Sweden, Sep. 2017.
- [47] G. Böcherer, F. Steiner, and P. Schulte, “Bandwidth efficient and rate-matched low-density parity-check coded modulation,” *IEEE Trans. Commun.*, vol. 63, no. 12, pp. 4651–4665, Dec. 2015.